VNU Journal of Science: Natural Sciences and Technology

Journal homepage: https://js.vnu.edu.vn/NST

Original Article

Green Synthesis of ZnO Nanoparticles using *Piper chaudocanum* L. Leaf Extract: Characterization and its Application in Pb (II) Adsorption

Truong Thi Thao[1,*], Khieu Thi Tam[1], Nguyen Thi Huong Thom[1], Nguyen Thuong Tuan[2]

[1]*University of Science, Thai Nguyen University, Tan Thinh, Thai Nguyen, Vietnam*
[2]*Institute of life sciences, Thai Nguyen University, Quyet Thang, Thai Nguyen, Vietnam*

Received 21 July 2021
Revised 13 November 2021; Accepted 13 November 2021

Abstract: In this study, Zinc oxide nanoparticles (ZnO NPs) were green synthesized using *Piper chaudocanum* L. (*PC*) leaf extract by sol-gel method and used as an adsorbent for the removal of Pb (II) ions from aqueous solution. The synthesized ZnO NPs were characterized by X-ray diffraction (XRD), field emission scanning electron microscopy (FESEM), Fourier transform infrared spectroscopy (FTIR), Ultraviolet - visible spectroscopy (UV-Vis) and Brunauer - Emmet - Teller (BET). The results revealed high purity and wurtzite hexagonal structure of ZnO NPs in the size range of 28-37 nm. The morphology of the ZnO NPs varies in different polycrystalline aggregates depending on the amount of extract used, from nanorods to NPs clusters with a BET surface area of 8.56 m^2g^{-1}. Pb (II) ion adsorption was investigated at different pH, contact time, initial metal ion concentration, adsorbent dose and temperature. ZnO NPs were synthesized using 30 mL *PC* leaf extract (ZS30) is the best Pb (II) absorbent. The adsorption isotherm was well described by Langmuir (at low concentration of Pb (II)) and Freundlich isotherm model (at higher concentration of Pb (II)). The adsorption process follows pseudo-second-order reaction kinetic with a high regression coefficient. The calculated thermodynamic parameters, ΔG_o (between - 8.699 and - 7.569 kJ/mol at 298 - 316 K), ΔH_o (-20.085 kJ/mol) showed that the adsorption of Pb (II) on ZS30 surface was feasible, spontaneous and exothermic, respectively. The first layer absorption is chemisorption while the next layers are physical adsorption.

Keywords: ZnO nanoparticles; Pb (II) adsorption; green synthesis.

1. Introduction

ZnO NPs is one of the most commonly used metal oxides due to their attractive properties such as biosafety, bio-compatibility [1], high chemical stability, high electrochemical coupling coefficient, broad range of radiation absorption and high photostability and non-toxicity. Therefore, ZnO NPs are used as antimicrobial agents, semiconducting materials, electronic materials, gas sensors, solar cells, photocatalyst, and adsorbents. A few reports showed that ZnO NPs could efficiently absorb heavy metals [2, 3], pharmaceutical drugs [4],

* Corresponding author.
E-mail address: thao.truong671@gmail.com

https://doi.org/10.25073/2588-1140/vnunst.5275

dyes [5], phosphate [6],… from aqueous systems. In which, heavy metal pollution, the consequence of rapidly developing industrial production globally, is causing serious consequences for human health and the sustainable development of the natural ecological environment.

ZnO NPs were synthesized by a variety of methods, such as precipitation in water solution or from microemulsions, hydrothermal, sol-gel, vapour deposition, mechanochemical processes and green synthesis with the diversity in shape, size and spatial structure [7-9]. As green synthesis is the simplest of all, eco-friendly, cost-effective, convenient, and least toxic [10-15], thus it has been of great interest for the past years. The green synthesis of ZnO NPs has been reported to use several biomaterials such as bacteria, fungi, algae, and plants. In addition, synthesized ZnO NPs by plant extracts have been reported to have more different shapes and sizes in comparison to other biomaterials. The plant extract with phytochemicals such as phenolic compounds, terpenoids, alkaloids, amino acids, and glycosides are reported as reducing, capping and stabilizing agents in the synthesis of ZnO NPs.

PC is a medicinal plant used in Vietnamese traditional medicine. It is often used to cure all kinds of poisons and cure weather diseases. *PC* belongs to *Piper* genus. *Piper* genus contains a variety of compounds such as alkaloids, flavonoids, steroids, terpenoids, and so on [16]. These compounds that could create complex with metal ions and play a role as reducing agents. In this study, we used *PC* leaf extract to synthesize ZnO NPs without using any chemicals and evaluated the adsorption activity to Pb (II) ion in solution, towards Pb (II) removal from water and wastewater.

2. Experimental Details

2.1. Materials

Zinc acetate dihydrate ($Zn(CH_3COO)_2.2H_2O$, ≥ 99%), 1000 ppm lead standard solution, sodium hydroxide (NaOH, ≥ 98%) and hydrochloric acid (HCl, 36.5 - 38%) were purchased from Merck, Germany. *PC* leaves were collected from Son La province. Distilled water (DW) was used as the solvent.

2.2. Preparation of Aqueous Extracts

PC leaves were washed and dried at 50 °C, and then grounded into powder. Next, 10 g of *PC* leaf powder was ultrasound extracted by 100 mL of distilled water for 1 hour at 60 °C. The extracts were centrifuged, filtered and then stored at 4 °C for further experiments.

2.3. Synthesis of ZnO NPs

ZnO NPs was green synthesized by sol-gel method which only used zinc acetate dihydrate and extract of *PC* leaves, without any other substances. V ml of aqueous extract of *PC* leaves (30, 45, 60 mL) was added drop by drop into zinc acetate solution (3.324 g/50 mL DW) at 70 °C under vigorously stirring for 60 min. Then, the solution was heated to 80 °C, keep stirring until a gel state (viscosity) is formed. The gel was dried to form xerogel powder at 80 °C by an oven. The xerogel was ground and calcined to 380 °C for 60 min (heating rate 200 °C/h). The obtained powder (ZS) was named according to the volume of extract and designated as ZS30; ZS45; ZS60. The same procedure was performed by oxalic acid solution instead of the aqueous extract used to prepare the ZnO NPs sample as a control.

2.4. Materials Characterization

The synthesized ZnO NPs were characterized by X-ray diffractometer (XRD, Max 18XCE, Japan, using a CuKα source (λ = 0.154056 nm)), field emission scanning electron microscopy (FESEM, Hitachi S-4800), Fourier transform infrared spectroscopy (FTIR Jasco FT/IR 4600), Ultraviolet - visible spectroscopy (UV-Vis NIRV 770) and Brunauer - Emmet - Teller (BET, TriStar 3000 V6.07).

2.5. Adsorption Experiments

Adsorption of Pb (II) on ZnO NPs was studied in the batch mode experiments. Optimized process parameters for metal adsorption include pH (2, 4, 5, 6, 7, 8), adsorbent dose (0.05; 0.1; 0.2; 0.5 g/L), metal ion concentrations (35, 75, 100, 150 ppm), contact time (to 120 min) and temperature (25 and 43 °C). To test pH, 0.1 M HCl or 0.1 M NaOH were used to adjust the solution

pH, 0.0025 g ZnO NPs were added to 25 mL of 75 ppm Pb (II) solution of determined pH, then, the flasks were shaken at 298 K for 2 h to reach equilibrium in shaking incubator, the solution was centrifuged, filtered. To study other factors, the experimental procedure was similar to m(g) ZnO NPs added to 150 mL of Pb (II) solution (with determined pH and concentration), shaken in shaking incubator and the solution was withdrawn at defined times (5, 15, 30, 60, 120 min) to determine the concentration of Pb (II) in solution by Atomic Absorption Spectrophotometer (AAS, Shimadzu 6300, Japan). The Pb (II) removal (h, %) and adsorption capacity (q, mg/g) was calculated by following equations:

$$h\ (\%) = \frac{C_o - C_t}{C_o} x100\% \quad (1)$$

$$q_e = \frac{C_o - C_e}{m} xV \quad (2)$$

Where C_o, C_t, C_e (mg/L, ppm) is the initial concentration, concentration at t (min) and at equilibrium of metals in solution, respectively; q_e (mg/g) is the amount of metal ions adsorbed onto adsorbent at equilibrium, V (L) is the volume of metal ions solution and m (g) is the mass of the adsorbent.

3. Results and Discussion

3.1. Characterization of ZnO Nanoparticles

The XRD spectra of prepared ZnO are shown in Fig. 1. The peaks were seen at around 31.6, 34.4, 36.1, 47.4, 56.5, 62.8, 66.3, 67.8, 69.0, 72.5 and 76.8, which can be assigned to diffraction from (100), (002), (101), (102), (110), (103), (200), (112), (201), (004) and (202) planes, respectively (PDF code no: 00-036-1451) [17]. No other phases or compounds than ZnO were observed in the samples. This revealed that the resultant nanoparticles were of pure ZnO with a hexagonal structure. The diffraction peaks of synthesized ZS become more intensified than those of synthesizing by oxalic acid. The higher the volume of extract used, the more the diffraction peaks slightly shift toward the lower value of 2 theta. The size of ZnO NPs has been calculated followed Debye-Scherrer equation [11]:

$$d = \frac{0.89\lambda}{\beta cos\theta} \quad (3)$$

where, 0.89 is Scherrer's constant, λ is the X-ray wave length equal to 1.54 Å, β is the full width at half maximum and θ is half the diffraction angle ((101) plane).

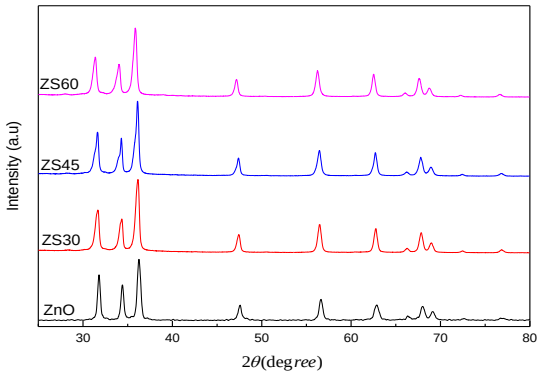

Figure 1. The XRD patterns of synthesized ZnO NPs.

The average particle size of the sample as calculated using equation (3) was found to be 32.0; 30.6; 33.5 and 36.0 nm for ZnO, ZS30, ZS45 and ZS60, respectively. It means that using 30 mL extract instead of oxalic acid reduces the particles size but at larger extract volumes (45, 60 mL), the particle size increased, possibly due to the excessive amount of extract, which increased the viscosity of the solution, reducing the diffusivity of the particles when they were formed, leading to an increase in particle size.

The typical FTIR spectrum of synthesized ZnO NPs is shown in Fig. 2. The FTIR spectra of all samples showed a broad absorption peak about 400–600 cm^{-1} which was assigned to the vibration of the Zn–O bond. In addition, other absorption bands appeared at 2365, 1580, 1490, and 1125 cm^{-1} characterized by stretching vibrations of OH group, C≡C bond, aromatic C=C bond, and C-O stretching modes, respectively. These signals are attributed to the functional groups present in the ZnO due to incomplete combustion of oxalic acid or organic substances in the extract at 380 °C. However, the signal intensity on the spectrogram decreases in the order: ZS30 > ZS45 > ZnO > ZS60, proving that the density of organic functional group that exists on the surface of ZS30 is the highest. The broad band

at 3450 cm^{-1} didn't appear in the FTIR spectrum of ZnO NPs synthesized by oxalic acid. It's because the surface of ZS is present in O-H bond that easier absorb moisture than ZnO. It menas that ZS surface can be more polarized than ZnO.

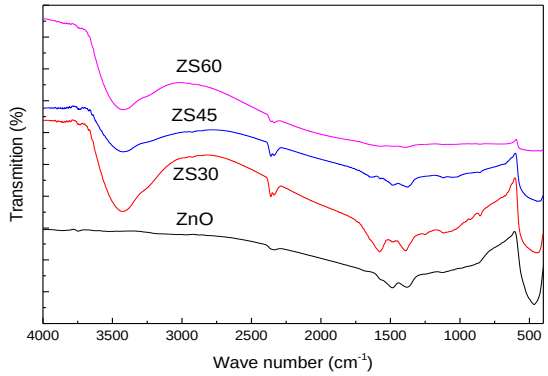

Figure 2. The IR patterns of synthesized ZnO NPs.

UV-Vis spectra were used to evaluate the optical performance of synthesized ZnO NPs samples. 0.5 mg ZnO NPs was dissolved in 25 mL of DW by ultrasonic vibration method, the absorbance of solution was measured. The results were shown in Fig. 3.

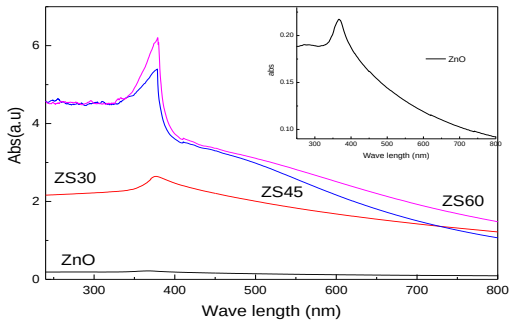

Figure 3. The UV-Vis absorption patterns of synthesized ZnO NPs.

The ZnO NPs absorption spectra demonstrated excitonic absorption edge at around 366 nm but the absorption peaks of ZS samples are shifted to 377.5 nm with a marked increase in peak intensity with increasing extract volume. ZnO synthesized by *Azadirachta indica* leaf extract [18] and *Solanum nigrum* leaf extract [13] showed the similar to previous results. The absorbance of ZS is higher than ZnO, increases as the extract volume increases from 30 to 45 mL but does not increase if the extract volume increases from 45 to 60 mL. It is possible that the extract encapsulating ZnO particles not only disperses the particles but also increases the solubility in water and increases the absorption capacity of ZnO.

The adsorption capacity mainly depends on the surface morphology of the adsorbent. Surface properties of ZS30 were investigated via nitrogen absorption-desorption experiments (Fig. 4). The isotherm Linear Plot was of type V, which indicated the meso-porous characteristics of ZS30 sample [14]. The BET surface area (m^2/g), total pore volume (cm^3/g) and mean pore diameter (nm) were 8.5634, 0.052413 and 31.3164 respectively. This result is the same as in other studies [19, 20].

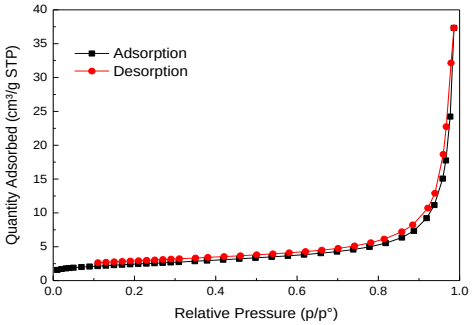

Figure 4. The BET surface area nitrogen adsorption-desorption isotherms of ZS30.

The morphology of the samples was assessed by scanning electron microscopy (SEM, Fig. 5). Fig. 5 a and 5 d are the SEM images of ZnO NPs (which was synthesized by oxalic acid), they were hexagonal in shape, the size was about 30 - 40 nm, and agglomerated into rod-shaped porous blocks, about 200 nm wide and from 500 to thousands nm long. The SEM images of ZS30 are shown in Fig. 5 b and 5 e, they were in nanorod shape, about 30 nm wide and 100 nm long; they were also agglomerated into porous triangular tower blocks, about 150 nm wide and 600 nm long. And ZS45 SEM images are on Fig. 5c and 5f, the particles return to hexagonal in shape but were not uniform in size, with particles as small as 40 nm and those as large as about 90 nm, they were also agglomerated into porous triangular tower blocks, same length as ZS30 but the bottom is twice as wide, rough surface by some scattered particles. The volume of extract strongly influenced the size and the shape of particles.

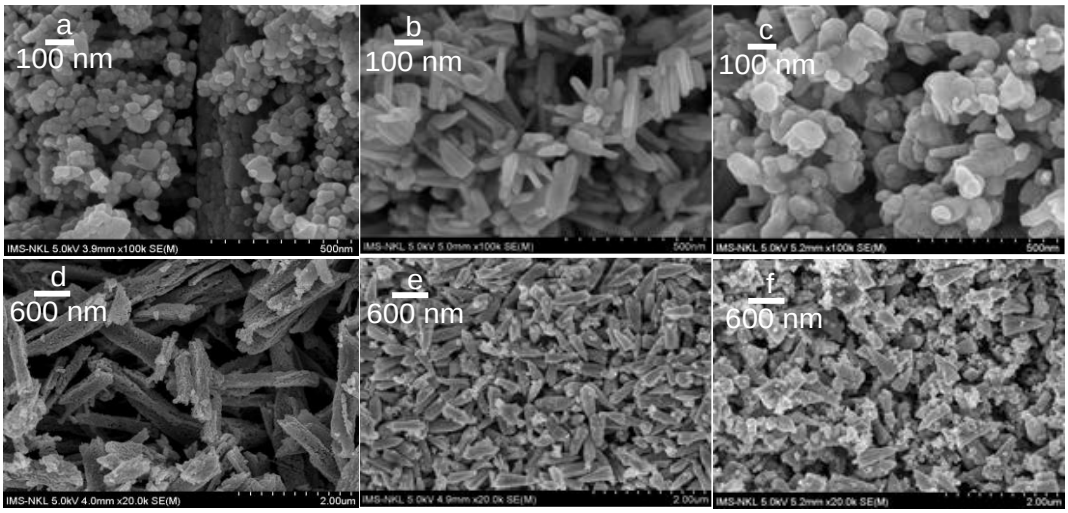

Figure 5. SEM images of (a), (d) ZnO; (b), (e) ZS30 and (c), (f) ZS45 samples.

3.2. Adsorption Studies

The Pb (II) adsorption capacity of synthesized ZnO was performed for varying contact times at pH 6, at concentration 75 ppm at 30 ◦C with 0. 1 g/L adsorbent. The results are shown in Figure 6a. At the initially contact time, the adsorption rate initially increased rapidly, and then adsorption equilibrium was reached after 60 min. The adsorption of ZnO is slightly lower than ZS sample, as the extract volume increased, the adsorption decreased. This result is completely consistent with the results of FTIR spectrum analysis of synthesized material: ZS30 is the smallest particle size and the largest hydrophilicity. So that, the ZS30 will be used in the following experiments.

The adsorption behavior of Pb (II) onto ZS30 has been investigated at different pHs ranging from 2.0 to 8.0 for initial Pb (II) concentration of 75 ppm, concentration of ZS30 was 0.1 g/L, the absorption after 60 min was shown in Fig. 6b. The adsorption of Pb (II) increased with increase in the solution pH from 2.0 to 6.0 and the adsorption decreased as pH keep increasing from 7.0 to 8.0. It is a commonly known fact that at a lower pH, the oxide surface will have positive character, less Pb (II) could be adsorbed because of electrostatic repulsion and there exists a competition between H^+ ions and Pb (II) ions. As the pH of solution increases, the surface protonation decreases and thus adsorbent surfaces were more negatively charged and the sorption of Pb (II) ions increased, reached maximum at pH 6.0. At pH > 6.0, the metal ions format the soluble hydroxylated complexes and their competition with the active sites. In addition, Pb (II) ions formed metal hydroxide and precipitate out. And as a consequence, the adsorption had been decreased. This result is similar with many previously published results [2, 3]. Therefore, all adsorption experiments were carried out at pH 6.

Effect of initial Pb (II) concentration (35 to 150 ppm) to the adsorption on 0.1 g/L ZS30 at pH 6, 30 ºC, and contact time ranging from 0 to 120 min was shown in Fig. 6c. The effect of amount of ZS30 on the adsorption of 75 ppm Pb (II) ions was examined in the range of 0.05 to 0.5 g/L at pH 6, 30 ºC, and contact time ranging from 0 to 120 min was shown in Fig. 6d. With increase in the amount of ZS30 and decrease in the initial Pb (II) concentration, percentage adsorption of Pb (II) ions was found to increase. This results will be used to study the adsorption isotherm modeling and kinetic modeling.

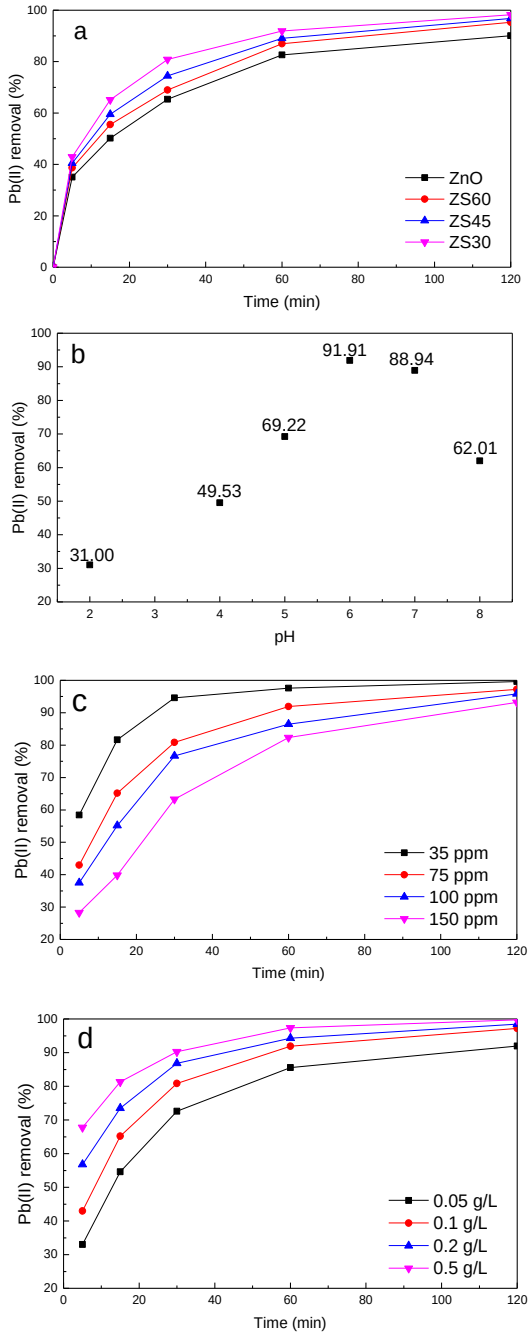

Figure 6. The adsorption of 75 ppm Pb (II) solution on the 0.1 g/L prepared ZnO samples (a) and on ZS30 at difference pH (b); The adsorption of difference initial concentration of Pb (II) solution on the 0.1 g/L ZS30 (c) and The adsorption of 75 ppm Pb (II) solution on the difference ZS30 dose (d) at pH 6, 30 °C.

Adsorption isotherm modeling:

Adsorption data has been subjected to Langmuir, Freundlich and Temkin models as they are the most common isotherms describing solid-liquid adsorption system. These three models are expressed as follows [5, 15]:

Langmuir isotherm model:

$$\frac{C_e}{q_e} = \frac{1}{K_L \cdot q_{max}} + \frac{C_e}{q_{max}} \quad (4)$$

Freundlich isotherm model:

$$\text{Log}(q_e) = \log(K_F) + \frac{1}{n}\log(C_e) \quad (5)$$

Temkin isotherm model:

$$q_e = B\lg K_T + B\lg C_e \quad (6)$$

where K_L (L/mg), K_F (L/mg) and K_T (L/mg) are the equilibrium adsorption constant for Langmuir, Freundlich and Temkin isotherm model, respectively, 1/n implies the degree of non-linearity between solution concentration and adsorption in Freundlich equation, B_1 is related to the heat of adsorption in Temkin equation. The fitting plots of these models are shown in Fig. 7. At the initial concentration of Pb (II) from 35 to 75 ppm, the correlation coefficients of Langmuir model are higher than those of Freundlich and Temkin equations; but at Pb (II) concentration from 100 to 150 ppm, the correlation coefficients of Freundlich model are higher than those of Langmuir and Temkin equations. It indicated that at low concentration of Pb (II), the experimental data agrees well with the Langmuir model (R^2 values are 0.98477 for 35 ppm Pb (II)) and 0.95242 for 75 ppm Pb (II) solution): the adsorption has not reached saturation, adsorption of Pb (II) ion from liquid solutions on the ZS30 surface is monolayer adsorption; at higher concentration of Pb (II), the experimental data are in good agreement with the Freundlich model (R^2 values are 0.98992 for 100 ppm Pb (II)) and 1 for 150 ppm Pb (II) solution), multilayer adsorption occurred. The multilayer adsorption process is essentially physical adsorption. Fig. 7 c also shown that, the maximum Pb (II) adsorption capacity q_{max} values of ZS30 is higher than some other reports [2, 3, 21, 22].

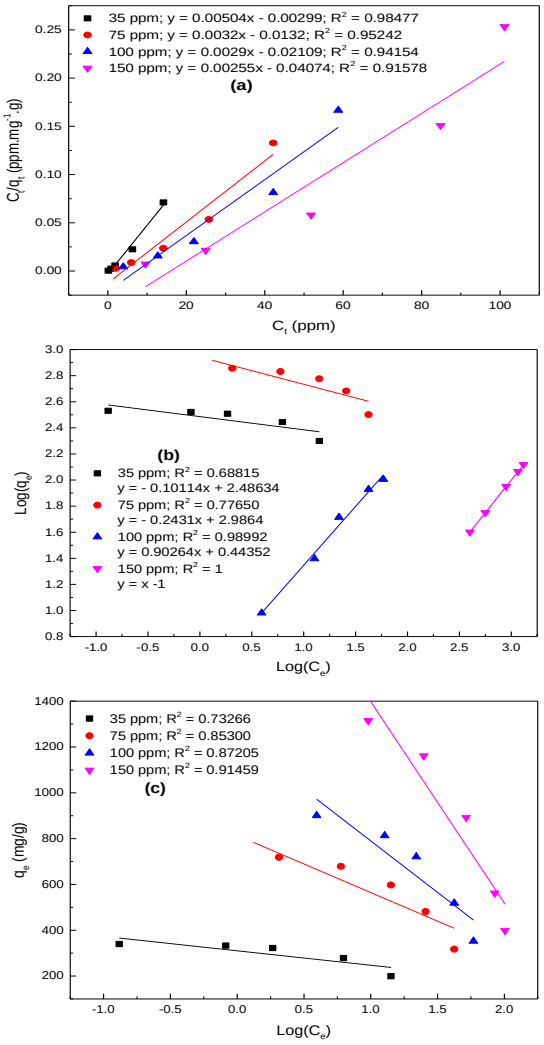

Figure 7. Adsorption isotherms for the adsorption of difference initial concentration of Pb (II) solution on 0.1 g/L ZS30 at pH 6, 30 °C.
(a) Langmuir isotherm model; (b) Freundlich isotherm model; (c) Temkin isotherm model.

Adsorption kinetic modeling:

The kinetics of Pb (II) adsorption onto ZS30 NPs was evaluated using three kinetics models, including pseudo first-order, pseudo-second-order and intra-particle diffusion models; their linear forms are given in equation (7), (8) and (9), respectively [3, 23]:

Pseudo- first -order kinetic model:

$$lg(q_e - q_t) = lgq_e - k_1.t \quad (7)$$

Pseudo-second-order kinetic model:

$$\frac{t}{q_t} = \frac{1}{k_2 q_e^2} + \frac{t}{q_e} \quad (8)$$

Intra-particle diffusion model:

$$q_t = k_{id} t^{0.5} + c \quad (9)$$

Where k_1 (min^{-1}), k_2 ($g/mg.min^{-1}$) and k_{id} ($mg/g.min^{-0.5}$) are the rate constants of the pseudo-first-order, pseudo-second-order, and intra-particle diffusion models, respectively; c is the intercept of the intra-particle diffusion model, $q_e = q_{120}$; The fitted plots of these adsorption kinetic models are shown in Fig. 8.

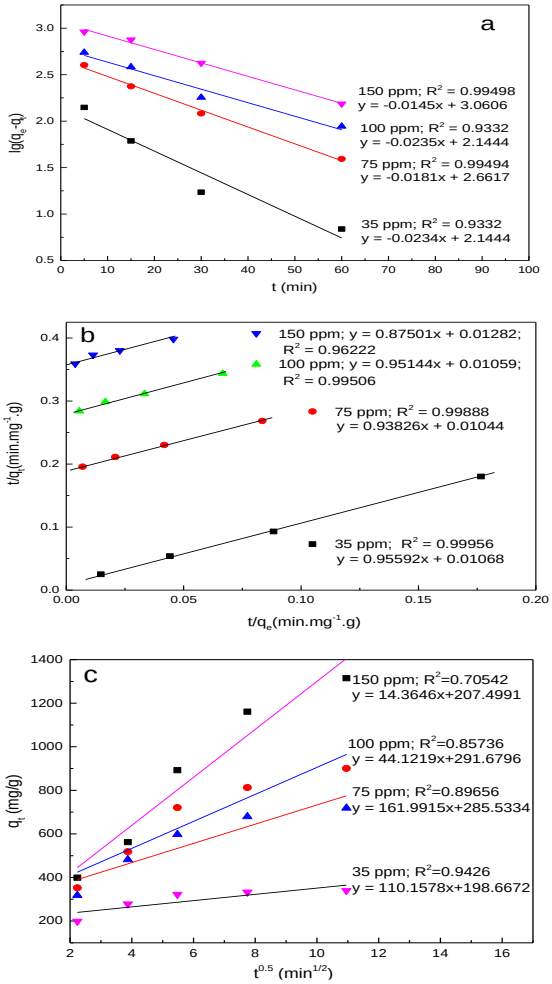

Figure 8. Kinetic models for adsorption of the different initial concentration of Pb (II) on 0.1 g/L ZS30-NPs surface at pH 6, 30 °C.
(a) Pseudo-first-order model; (b) Pseudo-second-order model; (c) Intra-particle diffusion model.

According to obtained results, the R^2 values of pseudo-second-order kinetic equation are the highest indicated that pseudo-second-order kinetic equation was well fitted to metal adsorption experiment. And it can be assumed that the adsorption system related electron sharing or electron transfer [5].

Thermodynamic:

Apparent equilibrium constant (distribution coefficient) (K_c), The enthalpy (ΔH), entropy (ΔS) and the Gibbs free energy of adsorption (ΔG) can be determined by the following equations [5]:

$$K_c = C_{eA}/C_e \quad (10)$$

$$ln\frac{K_{C,T_2}}{K_{C,T_1}} = \frac{\Delta H}{R}\left(\frac{1}{T_1} - \frac{1}{T_2}\right) \quad (11)$$

$$\Delta G = -RTlnK_c = \Delta H - T\Delta S \quad (12)$$

where R (8.314 J/mol K) is the universal gas constant, T (Kelvin) is the absolute temperature, C_{eA} (mg/L) is the concentration of Pb (II) ion on the adsorbent at equilibrium, C_e (mg/L) is the equilibrium concentration of Pb (II) ion on the solution.

Adsorption experiments were conducted at 298 and 316 K to investigate the effect of temperature, with initial Pb (II) concentration of 75 mg/L, adsorbent dosage of 0.1 g/L, pH 6 and contact time of 120 min. The results obtained K_{298} = 34.953; K_{316} = 22.028 and are used to calculate ΔH, ΔG, ΔS by in the following equations (10), (11) and (12). The negative ΔG values (ΔG_{298} = - 8.699 kJ/mol and ΔG_{316} = - 7.569 kJ/mol) indicate the spontaneous nature the adsorption of Pb (II) onto the ZS30 surface and the adsorption is more favorable at lower temperatures. The positive value of ΔH (20.085 kJ/mol) and ΔS (38.2 $J.mol^{-1}.K^{-1}$) reveals the Pb (II) adsorption onto the ZS30 is endothermic and takes place randomness at the solid-solution interface. ΔH is about 20 kJ/mol also shown that the first layer absorption dominated by chemisorption [24].

4. Conclusion

ZnO NPs were successfully synthesized by sol-gel method using *PC* leaf extract. The synthesized ZnO NPs have different shapes and sizes depending on the amount of extract. All ZS may adsorb Pb (II) from aqueous solution at pH 6 at room temperature higher than synthesized ZnO according to the traditional sol-gel method (using oxalic acid). The removal efficiency of Pb (II) from solution increases with the increase of adsorbent dose and decreases as the concentration of Pb (II) ion and temperature increase. The efficiency of removing Pb (II) from a 35 ppm solution by 0.1 g/L ZS30 or Pb (II) from a 75 ppm solution by 0.5 g/L ZS30 after 60 min was about 97%. The adsorption process of Pb (II) on the surface of ZS30 NPs was spontaneous, endothermic, follows the Langmuir isotherm model at low concentration of Pb (II) ion and follows the Freundlich isotherm model at high concentration of Pb (II) ion, and follows the pseudo-second-order reaction kinetic. The first layer absorption is chemisorption the next layers are physical adsorption.

References

[1] S. S. Sana et al., Crotalaria Verrucosa Leaf Extract Mediated Synthesis of Zinc Oxide Nanoparticles: Assessment of Antimicrobial and Anticancer Activity, Molecules, Vol. 25, No. 21, 2020.

[2] S. Azizi, M. M. Shahri, R. Mohamad, Green Synthesis of Zinc Oxide Nanoparticles for Enhanced Adsorption of Lead Ions from Aqueous Solutions: Equilibrium, Kinetic and Thermodynamic Studies, Molecules, Vol. 22, No. 6, 2017.

[3] N. Kataria, V. K. Garg, Optimization of Pb (II) and Cd (II) Adsorption Onto ZnO Nanoflowers using Central Composite Design: Isotherms and Kinetics Modelling, Ii. Elsevier B.V, 2018.

[4] N. Dhiman, N. Sharma, Removal of Pharmaceutical Drugs from Binary Mixtures by use of ZnO Nanoparticles: (Competitive Adsorption of Drugs), Environ, Technol, Innov., Vol. 15, 1019, pp. 100392.

[5] F. Zhang, X. Chen, F. Wu, Y. Ji, High Adsorption Capability and Selectivity of ZnO Nanoparticles for

Dye Removal, Colloids Surfaces A Physicochem, Eng, Asp., Vol. 509, 2016, pp. 474-483.

[6] B. Yan, Z. Hiew, L. Yee, X. Jiat, S. Gan, Equilibrium, Kinetic and Thermodynamic Studies, J. Taiwan Inst, Chem, Eng., Vol. 0,2018, pp. 1-13.

[7] C. Boon et al., A Review of ZnO Nanoparticles as Solar Photocatalysts : Synthesis, Mechanisms and Applications, Renew, Sustain, Energy Rev., Vol. 81, August 2017, pp. 536-551.

[8] M. Pirhashemi et al., Journal of Industrial and Engineering Chemistry Review on the Criteria Anticipated for the Fabrication of Highly Efficient ZnO-based Visible-light-driven Photocatalysts, J. Ind. Eng. Chem, Vol. 62, 2018, pp. 1-25.

[9] P. Raizada et al., Photocatalytic Water Decontamination using Graphene and ZnO Coupled Photocatalysts : A Review, Mater. Sci. Energy Technol, Vol. 2, No. 3, pp. 509-525, 2019.

[10] Z. Noohpisheh, H. Amiri, S. Farhadi, A. M. Gholami, Green Synthesis of Ag-ZnO Nanocomposites using Trigonella Foenum-graecum Leaf Extract and their Antibacterial, Antifungal, Antioxidant and Photocatalytic Properties, Spectrochim, Acta - Part A Mol. Biomol. Spectrosc., Vol. 240, 2020, pp. 118595.

[11] C. A. Soto-Robles et al., Study on the Effect of the Concentration of Hibiscus Sabdariffa Extract on the Green Synthesis of ZnO Nanoparticles, Results Phys., Vol. 15, 2019, pp. 102807.

[12] W. Ahmad, D. Kalra, Green Synthesis, Characterization and Anti Microbial Activities of ZnO Nanoparticles using Euphorbia Hirta Leaf Extract, J. King Saud Univ. - Sci., Vol. 32, No. 4, 2020, pp. 2358-2364.

[13] A. Muthuvel, M. Jothibas, C. Manoharan, Effect of Chemically Synthesis Compared to Biosynthesized ZnO-NPs using Solanum Nigrum Leaf Extract and Their Photocatalytic, Antibacterial and In-vitro Antioxidant Activity, J. Environ. Chem. Eng., Vol. 8, No. 2, 2020, pp. 103705.

[14] A. Bayrami, S. Haghgooie, S. R. Pouran, F. M. Arvanag, A. H. Yangjeh, Synergistic Antidiabetic Activity of ZnO Nanoparticles Encompassed by Urtica Dioica Extract, Adv, Powder Technol., Vol. 31, No. 5, 2020, pp. 2110-2118.

[15] M. Khatami, R. S. Varma, N. Zafarnia, H. Yaghoobi, M. Sarani, V. G. Kumar, Applications of Green Synthesized Ag, ZnO and Ag/ZnO Nanoparticles for Making Clinical Antimicrobial Wound-healing Bandages, Sustain, Chem. Pharm., Vol. 10, 2018, pp. 9-15.

[16] B. Salehi et al., Piper Species: A Comprehensive Review on Their Phytochemistry, Biological Activities and Applications, Vol. 24, No. 7, 2019.

[17] A. K. Zak, R. Razali, W. H. A. Majid, M. Darroudi, Synthesis and Characterization of a Narrow Size Distribution of Zinc Oxide Nanoparticles, Int. J. Nanomedicine, Vol. 6, No. 1, 2011, pp. 1399-1403.

[18] T. Bhuyan, K. Mishra, M. Khanuja, R. Prasad, A. Varma, Biosynthesis of Zinc Oxide Nanoparticles from Azadirachta Indica for Antibacterial and Photocatalytic Applications, Mater. Sci. Semicond. Process., Vol. 32, 2015, pp. 55-61.

[19] A. N. Kadam et al., Facile Synthesis of Ag-ZnO Core-shell Nanostructures with Enhanced Photocatalytic Sctivity, J. Ind. Eng. Chem., Vol. 61, 2018, pp. 78-86.

[20] A. Modwi, M. A. Ghanem, A. M. A. Mayouf, A. Houas, Lowering Energy Band Gap and Enhancing Photocatalytic Properties of Cu/ZnO Composite Decorated by Transition Metals, J. Mol. Struct., Vol. 1173, 2018, pp. 1-6.

[21] V. Venkatesham, G. M. Madhu, S. V. Satyanarayana, H. S. Preetham, Adsorption of Lead on Gel Combustion Derived Nano ZnO, Procedia Eng., Vol. 51, 2013, pp. 308-313.

[22] S. Z. N. Ahmad et al., Pb(II) Removal and its Adsorption from Aqueous Solution using Zinc Oxide/graphene Oxide Composite, Chem. Eng. Commun., Vol. 208, No. 5, 2021, pp. 646-660.

[23] K. Nalwa, Synthesis of ZnO Nanoparticles and its Application in Adsorption, Adv. Mater. Proc., Vol. 2, No. 11, 2017, pp. 697-703.

[24] M. N. Zafar, Q. Dar, F. Nawaz, M. N. Zafar, M. Iqbal, M. F. Nazar, Effective Adsorptive Removal of Azo Dyes Over Spherical ZnO Nanoparticles, J. Mater. Res. Technol., Vol. 8, No. 1, 2019, pp. 713-725.